

Collimation of extragalactic radio jets in compact steep spectrum and larger sources

S. Jeyakumar[★] and D.J. Saikia[†]

National Centre for Radio Astrophysics,

Tata Institute of Fundamental Research, Ganeshkhind, Pune 411007, India

ABSTRACT

We study the collimation of radio jets in the high-luminosity Fanaroff-Riley class II sources by examining the dependence of the sizes of hotspots and knots in the radio jets on the overall size of the objects for a sample of compact steep-spectrum or CSS and larger-sized objects. The objects span a wide range in overall size from about 50 pc to nearly 1 Mpc. The mean size of the hotspots increases with the source size during the CSS phase, which is typically taken to be about 20 kpc, and the relationship flattens for the larger sources. The sizes of the knots in the compact as well as the larger sources are consistent with this trend. We discuss possible implications of these trends. We find that the hotspot closer to the nucleus or core component tends to be more compact for the most asymmetric objects where the ratio of separations of the hotspots from the nucleus, $r_d > 2$. These highly asymmetric sources are invariably CSS objects, and their location in the hotspot size ratio - separation ratio diagram is possibly due to their evolution in an asymmetric environment. We also suggest that some sources, especially of lower luminosity, exhibit an asymmetry in the collimation of the oppositely-directed radio jets.

Key words: galaxies: active - galaxies: nuclei - galaxies: jets - quasars: general - radio continuum: galaxies

1 INTRODUCTION

It is well established that energy is supplied more or less continuously to the outer lobes by beams of plasma ejected from the nucleus at relativistic speeds. The radio jets, which are the signatures of these energy-carrying beams, expand rapidly with distance from the nucleus for the low-luminosity FRI sources (Fanaroff & Riley 1974), but are highly collimated and less dissipative in the high-luminosity FRII objects (cf. Bridle & Perley 1984). However, jets in both these classes show evidence of flaring and recollimation on different scales (cf. Hardee, Bridle & Zensus 1996). The transverse widths of the knots, Φ , tend to increase with distance, Θ , from the central or nuclear component. However, the increase is not linear as would be expected in a freely expanding jet. The spreading rate, defined to be the ratio Φ/Θ , is usually larger close to the nucleus, which is followed by a slower spreading rate or recollimation. Some examples of well-studied jets in the high-luminosity FRII sources are the ones in the 3CR quasars studied by Bridle et al. (1994, here-

inafter referred to as B94), the N galaxy 3C390.3 by Leahy & Perley (1995), the radio galaxies Cygnus A (cf. Carilli et al. 1996) and 3C353 (Swain, Bridle & Baum 1996). The transverse knot widths in the inner jet in the quasar 3C351 suggest a high spreading rate of 0.13, while the outer jet is better collimated. The jets in the quasars 3C204, 3C263 and 3C334 exhibit faster than average spreading rate when they are closest to the nucleus. The knots in the jets in 3C175 and 3C334 exhibit a decrease in their transverse widths before entering the hotspots, while the jets in the quasars 3C204 and 3C263 show evidence of flaring before entering the hotspots (B94). In the N galaxy 3C390.3, the width of the jet is almost constant from 30 to 120 kpc, it decreases till about 180 kpc and then increases again before entering the hotspot (Leahy and Perley 1995). The width of the extended jet in the radio galaxy 3C353 remains roughly constant beyond about 20 kpc (Swain et al. 1996). Evidence of recollimation are also seen in the small-scale nuclear jets. For example, in the compact steep-spectrum quasar 3C138, Fanti et al. (1989) have reported evidence of recollimation of the jet on scales of less than few hundred pc. The nuclear jet in Cygnus A has a width of about 2.2 mas over a distance ranging from 2 to 20 mas from the nucleus (Car-

[★] E-mail: sjk@ncra.tifr.res.in

[†] E-mail: djs@ncra.tifr.res.in

illi et al. 1996). These observations suggest that radio jets are often confined on scales ranging from the nuclear jets on the scale of parsecs to the extended ones on scales of hundreds of kpc. The jets could be pressure confined by the external environment or by magnetic fields around the jets (cf. Sanders 1983; Bridle & Perley 1984; Appl & Camenzind 1992, 1993a,b; Appl 1996; Kaiser & Alexander 1997).

In this paper, we concentrate on the hotspots and radio knots in the jets and use their sizes over a large range of source sizes to investigate the collimation of jets in the compact steep spectrum and larger sources. The hotspots indicate the Mach disks where the jets terminate and subtend small angles in the radio cores suggesting the high degree of collimation of the jets in these sources (Bridle & Perley 1984; B94; Fernini, Burns & Perley 1997, hereinafter referred to as F97). Inclusion of hotspots enables us to study the collimation of jets for a large sample of sources independent of whether a jet has been detected and its transverse width determined. However, the jet momentum may be spread over a larger area than the cross-section of the jet itself due to the dentist-drill effect discussed by Scheuer (1982), where the end of the jet wanders about the leading contact surface drilling into the external medium at slightly different places at different times. Recent simulations of 3D supersonic jets suggest that cocoon turbulence drives the dentist-drill effect (Norman 1996).

Over the last few years the sizes of hotspots have been determined for samples of compact steep-spectrum radio sources using largely VLBI and MERLIN observations, as well as for the larger objects using the VLA. Although there is no well-accepted definition of a hotspot (cf. Laing 1989; Perley 1989), we are interested in features which mark the collimation of jets and have used the following empirical definition. The hotspots are defined to be the brightest features in the lobes located further from the nucleus than the end of any jet, and in the presence of more extended diffuse emission these should be brighter by at least a factor of about 4 (cf. B94). In the presence of multiple hotspots, only the primary hotspot has been considered. The jets which we consider have been well-mapped and follow the defining criteria suggested by Bridle & Perley (1984). We have used the information on the sizes of the hotspots and the widths of the knots in the jets to study the collimation and expansion of the radio jets over a wide range of angular and linear scales. The overall linear sizes of our objects are spread over about 5 orders of magnitude ranging from about 50 pc to nearly 1 Mpc.

2 SAMPLE OF SOURCES

Our sample has been chosen from well-defined samples of compact and larger sources which have been observed with high angular resolution. We have compiled our sample of compact sources from the following samples of CSS and Gigahertz Peaked Spectrum or GPS sources: (i) the sample of 67 sources listed by O’Dea (1998) and O’Dea & Baum (1997) which is based on the Fanti et al. (1990) CSSs and Stanghellini et al. (1990, 1996) GPS objects; (ii) the Sanghera et al. (1995) compilation of 62 objects, which consists of all sources from the complete samples of 3C (Fanti et al. 1990), PW (Peacock & Wall 1982) and a Jodrell-Bank

sample; and (iii) the 7 confirmed compact symmetric objects or CSOs listed by Taylor, Vermeulen & Pearson (1995) and Taylor, Readhead & Pearson (1996). Our resulting combined sample consists of 86 objects, because there are many sources which are common to the above lists, and have been counted only once in our combined list. Of these 86, we have considered those which have a well-defined double-lobed structure and where the hotspot sizes are available or could be determined. Sources with a complex and highly distorted structure have been excluded. Typical examples of such sources are 3C48 (Wilkinson et al. 1991) and 3C119 (Ren-dong et al. 1991a). In addition, we have excluded the source 0319+121 which has been listed as a GPS object by Stanghellini et al. (1990), but single-epoch observations of the nucleus from 1.4 to 15 GHz show that it has a flat radio spectrum (Saikia et al. 1998). A few of our sources, such as 0108+388 (Baum et al. 1990), have extended emission in addition to the compact double or triple structure closer to the nucleus. The extended emission must be due to earlier periods of activity, with the luminosity and size of the component being governed by ageing and expansion of the component. On the other hand, the compact structure closer to the nucleus represent more recent activity with the size of the hotspots indicating the degree of collimation of the jets. Hence, in such cases we have considered only the compact double or triple structure.

The sample which consists of 58 objects at this stage has been further restricted to those which have been observed with at least 10 resolution elements, n_b , along the main axis. We also focus on the subsample which has been observed with $n_b \geq 20$, for a more reliable estimation of the hotspot parameters. In our entire sample only 6 lobes have no hotspots which meet our defining criteria. Excluding these lobes does not affect any of the conclusions presented in this paper. Sources which were earlier classified as CSS objects but were later found to be of larger dimensions have not been excluded from the sample. Our final sample of largely CSS and GPS objects consists of 39 sources, 9 of which are >20 kpc. This sample is listed in Table 1, which is arranged as follows: columns 1 and 2: source name and an alternative name; column 3: optical identification where G denotes a galaxy, Q a quasar and EF an empty field; column 4: the sample where O, S and T denote O’Dea & Baum (1997) and O’Dea (1998), Sanghera et al. (1995) and Taylor et al. (1995, 1996) respectively; column 5: redshift; column 6: the structural classification of the source where D denotes a double, T a triple with a radio core, and T? a triple with a possible core component; column 7: the angular separation of the hotspots on opposite sides of the nucleus, expressed in arcsec; column 8: the corresponding linear size in kpc in an Einstein-de Sitter Universe with $H_0=50 \text{ km s}^{-1} \text{ Mpc}^{-1}$; column 9: the number of resolution elements, n_b , along the longest axis of the source, which is the largest angular size of the radio source divided by the size of the restoring beam along the axis of the source; columns 10 and 11: the major and minor axes of one hotspot in mas; columns 12 and 13: the major and minor axes for the other hotspot in mas; column 14 : ratio of the separation of the farther component from the radio core to the nearer one for those classified as T or T?; column 15: references for radio structure. For sources with a radio core, the size of the hotspot farther from the nucleus is listed in columns 10 and 11. The hotspot sizes

Table 1. The sample of largely CSS and GPS sources

IAU name	Alt. name	Id	Sample	z	St	LAS	Size	n_b	Hotspot sizes				r_d	Ref
									Hotspot 1		Hotspot 2			
(1)	(2)	(3)	(4)	(5)	(6)	arcsec	kpc		mas	mas	mas	mas	(14)	(15)
0108+388	OC+314	G	O,T	0.669	T	0.0058	0.054	12	0.47	0.23	0.53	0.39	1.34	1
0138+138	3C 49	G	O,S	0.621	T	1	9	14	100	40	20	10	2.42	2
0221+276	3C 67	G	O,S	0.310	T	2.47	15	41	160	60	115	98	2.45	2
0223+341	4C+34.07	Q?	O,S		D	0.546		18	* 30	26	* < 30	< 30		4
0404+768	4C76.03	G	O,S,T	0.599	T?	0.11	0.97	11	* 10	10	* 10	8	1.64	5,4
0428+205	OF247	G	O,S	0.219	T?	0.212	1	21	* 17	10	* 11	7	4.68	4
0518+165	3C 138	Q	O,S	0.759	T	0.615	6	12	* 71	37	* 64	25	1.72	18
0538+498	3C 147	Q	O,S	0.545	T	0.64	5.4	32			* 70	49	2.50	17
0707+689	4C+68.08	Q	S	1.139	T	1.18	13	19	170	100			1.24	2
0710+439	OI+417	G	O,T	0.518	T	0.025	0.21	25	1.08	0.63	0.48	0.13	1.12	1
0740+380	3C 186	Q	O,S	1.063	T	2.19	24	26	* 311	145	* 94	50	1.29	9
0758+143	3C 190	Q	O,S	1.197	T	2.6	30	76	* 101	76	* 89	76	1.61	9
0802+103	3C 191	Q	S	1.956	T	4.6	59	42	* 248	154	* 160	85	1.75	6,11,2
0858+292	3C 213.1	G	S	0.194	D	5.95	26	20	300	200	200	200		3
1019+222	3C 241	G	O,S	1.617	T	0.81	10	12	60	30	60	30	1.33	2,8
1031+567	OL+553	G	O,T	0.459	D	0.0334	0.26	24	* 1.7	1.5	* 1.5	1.1		1
1117+146	4C+14.41	G	O,S	0.362	D	0.08	0.54	11	15	7	20	6		2
1122+195	3C 258	G	S	0.165	D	0.1	0.38	14	15	10	15	8		2
1143+500	3C 266	G	S	1.275	D	4.16	49	14	500	100	700	300		3
1203+645	3C 268.3	G	O,S	0.371	T	1.36	9.3	13	190	110	118	81	3.06	12,2
1225+368	ON343	Q	O,S	1.974	T?	0.055	0.71	18	* < 7	3.2	* < 7	4	1.21	4
1244+492	4C+49.25	G	S	0.206	T	2.64	12	33	125	90	230	160	1.63	2
1250+568	3C 277.1	Q	O,S	0.321	T	1.7	11	57			* 50	37	2.55	2
1323+321	4C+32.44	G	O,S	0.370	D	0.055	0.37	11	* 10	6	* 9	3		4
1328+307	3C 286	Q	O,S	0.849	T	3.2	33	11	600	300	200	200	3.36	3,2
1402+660	4C+66.14	EF	S		T	0.17		24			26	12	1.37	2
1416+067	3C 298	Q	O,S	1.439	T	1.5	18	19	130	130	90	90	2.70	8
1419+419	3C 299	G	S	0.367	T	11.5	78	10	* 824	779	* 824	576	3.21	16,12
1447+771	3C 305.1	G	O,S	1.132	T?	2.34	27	16	149	119	89	46	2.40	8,2
1517+204	3C 318	G	O,S	0.717	T?	0.724	7	21	* 72	48	90	35	1.41	9
1518+047	4C+04.51	G	O	1.296	D	0.135	1.6	23	< 3.6	< 3.6	1.7	1.7		13,14
1607+268	CTD93	G	O,S	0.473	D	0.05	0.39	30	0.51	0.51	4.95	2.23		10
1946+708	TXS	G	T	0.101	T	0.031	0.079	24	5.04	0.76	0.93	0.69	1.00	15
2128+048	PKS	G	O	0.990	T	0.035	0.38	12	3.2	2.9	3.2	1.6	1.44	7
2210+016	4C+01.69	G?	O		T?	0.075		17	5.1	2.9			1.85	7
2252+129	3C 455	Q	O,S	0.543	D	3.12	26	10	* 871	673	800	400		3
2323+435	OZ438	G	S	0.145	T?	1.61	5.6	20	140	90	110	90	2.04	2
2342+821	S5	Q	O,S	0.735	T?	0.16	1.6	13	* 17	15	* 17	12	1.39	4
2352+495	OZ+488	G	O,T	0.237	T	0.049	0.25	55	2.06	1.26	1.2	0.83	1.05	1

References: 1. Taylor et al. 1996; 2. Sanghera et al. 1995; 3. Spencer et al. 1989; 4. Dallacassa et al. 1995; 5. Polatidis et al. 1995; 6.

Cawthorne et al. 1986; 7. Stanghellini et al. 1997; 8. van Breugel et al. 1992; 9. Spencer et al 1991; 10. Fey & Charlot 1997; 11.

Pearson, Perley & Readhead 1985; 12. Rendong et al. 1991b; 13. Mutel, Hodges & Phillips 1985; 14. Phillips & Mutel 1981; 15. Taylor, Vermeulen & Pearson 1995; 16. Liu, Pooley & Riley 1992; 17. Simon et al. 1990; 18. Akujor et al. 1993.

refer to the full width at half maximum. For some of the images where the authors quote the size of the entire component from the lowest reliable contour, we have estimated the sizes of the hotspots from the images. These have been marked with an asterisk in the Table.

For comparison with larger sources we consider those which have been observed with a similar number of resolution elements, n_b , along the main axis of the source. The comparison sample has been compiled from the complete sample of 3CR sources (Laing, Riley & Longair 1983) and consists of the FRII sources which have been observed with n_b between about 10 and 40. These limits were chosen so that the distribution of n_b is similar to the CSS and GPS objects. For the 3CR sources observed with the Cambridge

5-km telescope we have confined ourselves to sources above a declination of 30° so that the beams are not very elliptical. This sample is listed in Table 2 which is arranged similarly to Table 1 except for the following differences. These are all triples from the 3CR sample, and hence the sample column and structural information have been omitted.

In addition, we discuss briefly the collimation of jets using sources which have been observed with a larger number of resolution elements along their axes. These have been observed with high resolution and sensitivity with the Very Large Array (VLA) by B94, Fernini et al. (1993), F97, Black et al. (1992), Leahy et al. (1997), and Hardcastle et al. (1997, 1998). These observations give us estimates of the sizes of hotspots in larger sources. B94 have reported obser-

Table 2. The sample of large 3CR sources

IAU name	Alt. name	Id	z	LAS	Size	n_b	Hotspot sizes				r_d	Ref
							Hotspot 1		Hotspot 2			
							mas	mas	mas	mas		
(1)	(2)	(3)	(4)	arcsec	kpc	(7)	(8)	(9)	(10)	(11)	(12)	(13)
0013+790	3C 6.1	G	0.840	26	266.3	13	1300	< 900	< 900	< 900		2
0017+154	3C 9	Q	2.012	14	181.1	39	900	280	620	360	1.52	9
0040+517	3C 20	G	0.174	53	211.4	26	1700	2000	<1000	1700		5,1
0048+509	3C 22	G	0.936	24	255.8	12	<1000	1300	<1000	1300		1
0107+315	3C 34	G	0.690	48	453.4	24	1700	2300				1
0229+341	3C 68.1	Q	1.238	53	616.5	15	1500	1400				5,9
0605+480	3C 153	G	0.277	7.1	39.9	27	110	70	190	80	2.00	8
0702+749	3C 173.1	G	0.292	60	349.6	29	2500	1800	3600	2400	1.18	1
0809+483	3C 196	Q	0.871	5.5	57.1	22	700	500	500	150	1.32	7
0833+654	3C 204	Q	1.112	31.1	350.7	16	1500	<1000	2000	<1000		2,5
0835+580	3C 205	Q	1.534	16	196.3	20	< 300	< 400	< 400	< 500		5,2
0850+140	3C 208	Q	1.110	14	157.8	38	260	210	240	210	1.30	9,5
0926+793	3C 220.1	G	0.610	30	267.8	15	<1000	2000				1
1009+748	4C+74.16	G	0.200	40	177.6	19	500	700	2500	2000	1.41	6
1030+585	3C 244.1	G	0.428	53	392.6	23	1000	1200	1000	2000	1.15	1,5
1100+772	3C 249.1	Q	0.311	23	139.8	11	1300	1000	1300	<1000		2
1108+359	3C 252	G	1.105	60	675.3	28	<1000	1700				1
1111+408	3C 254	Q	0.734	13.2	128.0	19	< 200	< 300	< 200	< 300		5,2
1137+660	3C 263	Q	0.656	44.2	408.2	22	<1000	<1000				2
1142+318	3C 265	G	0.811	78	788.0	35	2200	1500	1100	2100	1.50	1,5
1157+732	3C 268.1	G	0.970	46	496.3	22	<1000	<1000	<1000	<1000		1,5
1254+476	3C 280	G	0.996	12.9	140.4	19	< 200	< 300	< 200	< 300		5,2
1533+557	3C 322	G	1.681	33	412.9	14	1100	1600	1800	<1000		1
1609+660	3C 330	G	0.550	62	526.0	30	1100	<1000	3300	<1000		1,5
1627+444	3C 337	G	0.630	43	389.7	21	<1000	<1500	1300	<1500		1
1658+471	3C 349	G	0.205	82	371.0	33	1600	1700				1,5
1704+608	3C 351	Q	0.371	64	435.3	29	1500	1000				3,9
1723+510	3C 356	G	1.079	75	837.9	29	<1000	1900	1600	<1500		1
1832+474	3C 381	G	0.161	69	258.9	26	<1500	<1000	6000	3000		3,5
2104+763	3C 427.1	G	0.572	23.1	199.9	11	5700	2300	2900	1500	1.01	2
2120+168	3C 432	Q	1.805	13.4	170.0	36	310	160	260	230	1.46	9
2352+796	3C 469.1	G	1.336	74	878.4	37	< 900	1300	< 900	2200		4

References: 1. Jenkins, Pooley & Riley 1977; 2. Pooley & Henbest 1974; 3. Riley & Pooley 1975; 4. Longair 1975; 5. Laing 1981; 6. Laing, Riley & Longair 1983; 7. Lonsdale & Morison 1983; 8. Hardcastle et al. 1998; 9. Bridle et al. 1994.

vations of 13 quasars while F97 have listed hotspot sizes for 9 galaxies. Hardcastle et al. (1998, hereinafter referred to as H98) have summarized the properties of jets, cores and hotspots in the sample of FRII galaxies with redshift < 0.3 which have been observed by the Cambridge group. In addition to the hotspots we have also considered the sizes of the knots in the jets listed in Table 9 of B94 and of the knots in the CSOs observed by Taylor et al. (1995, 1996).

3 COLLIMATION OF RADIO JETS

In the upper-left panel of Figure 1, we plot the angular sizes of the major and minor axes of each hotspot against the largest angular separation of each source in Tables 1 and 2, while on the upper-right panel we present the equivalent linear sizes for the same sources. The lower panels show the same plots but only for those sources which have been observed with at least about 20 resolution elements along the long axis of the source. Since we sometimes do not have information on the radio core, especially for the CSS and GPS objects we have plotted the hotspot sizes against the overall separation of the oppositely-directed hotspots. In this

figure, we have also plotted the knots in the CSOs imaged by Taylor et al. (1995, 1996). In this paper, we have made the least-squares fits to the hotspots by taking the average hotspot size for each source. This is defined to be the geometric mean of each hotspot and, for those with hotspots on both sides, the average of the two oppositely-directed hotspots for each source. As mentioned earlier, a distance of 20 kpc was chosen as the canonical limit for the size of the CSS and GPS objects (cf. Fanti et al. 1990; O’Dea 1998). A linear least-squares fit to the hotspots for the CSS and GPS objects in Figure 1 observed with at least 10 resolution elements shows that if the jet width is expressed as $d_{jet} = kl^n$, then $n \sim 1.02 \pm 0.06$ and $\log(k) \sim -1.23 \pm 0.05$. For those observed with at least 20 resolution elements the value of n is 1.10 ± 0.07 and $\log(k) \sim -1.4 \pm 0.05$. The sizes of the knots in the CSOs are consistent with this trend. There appears to be a well-defined relationship with the hotspot size increasing with the total size of the source upto a distance of about 20 kpc, the canonical limit for the sizes of CSSs. The sizes of the knots in the jets are similar to those of the hotspots. This relationship is consistent with self-similar

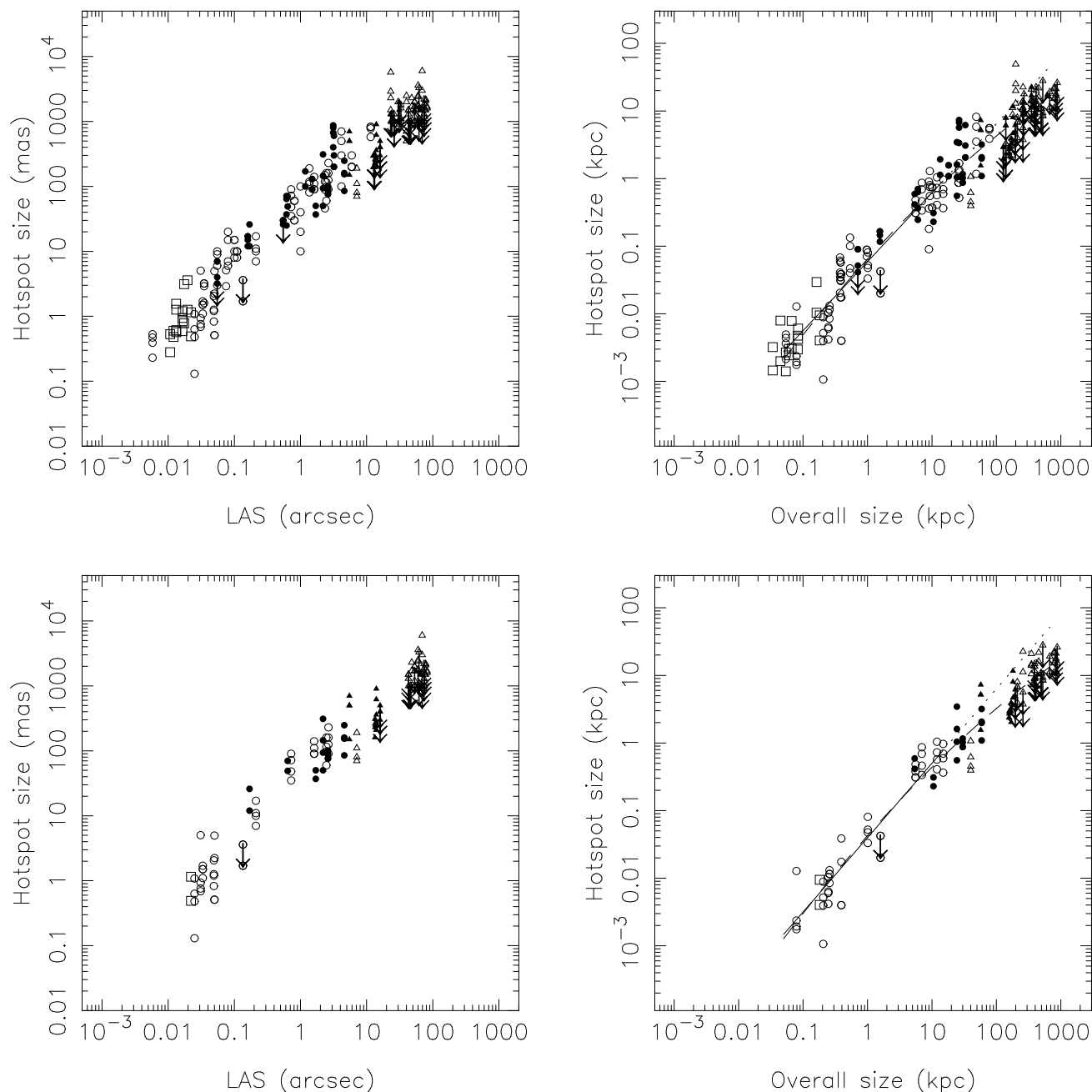


Figure 1. The size of each hotspot is plotted against the largest angular size of each source defined to be the separation of the oppositely-directed hotspots. Filled circles indicate quasars while open circles denote radio galaxies from the sample of largely CSS and GPS objects (Table 1). The knots in the jets of the compact symmetric objects are denoted by open squares. The hotspot sizes of the 3CR sources described in the text (Table 2) are indicated by open and filled triangles for the galaxies and quasars respectively. The arrows indicate upper limits. The upper panels indicate all sources observed with at least 10 resolution elements along the main axes while the lower panels show those which have been observed with at least 20 resolution elements along the main axes. The solid lines denote the linear least-squares fit to the average hotspot size for CSS and GPS sources, defined to be those below 20 kpc. These linear fits have been extended beyond 20 kpc by a dotted line to highlight the flattening of the relationship for larger sources. The dashed lines denote the parabolic fit to the average hotspot size of the sources in both the samples. For sources with upperlimits, the hotspot sizes have been estimated by assuming the true values to be close to the limits.

models for the evolution of radio sources during the CSS and GPS phase (cf. Kaiser & Alexander 1997).

3.1 Comparison with larger 3CR sources observed with similar resolution elements

To investigate this relationship for sources > 20 kpc, we have compared the CSS and GPS sources (Table 1) with the sample of 3CR sources (Table 2) which have been observed with similar resolution relative to the largest angular size as used for the CSS sources. The number of resolution elements, n_b , for the CSS sources vary from about 10 to 77 with a median value of about 19 while for the 3CR sources n_b ranges from about 10 to 39 with a median value of about 23. Only 5 of the CSSs have $n_b > 40$. Considering the sources which have been observed with n_b between about 20 and 40, the median values of n_b for CSS and GPS, and 3CR sources are 25 and 28 respectively, and a Kolmogorov-Smirnov test shows that the two distributions are the same with a probability of 66 per cent. The redshifts of the CSS and GPS sources range from about 0.1 to 2 with a median value of about 0.6 while the redshifts for the 3CR sample is somewhat larger ranging from about 0.16 to 2.0, with a median value of about 0.8.

The extension of the linear least-squares fit to the CSS sources beyond 20 kpc shows that most of the larger sources observed with a similar value of n_b lie below this line, suggesting a flattening of this relationship. This indicates recollimation of the jets beyond ~ 20 kpc. Since most of the measured sizes are upper limits, it is difficult to determine the precise nature of the relationship from the present sample. Assuming that the sizes of the hotspots with upper limits are close to these limits, we have attempted a linear least-squares as well as a parabolic fit to the entire data. The parabolic fits are significantly better, suggesting again a flattening of the relationship. To confirm the trend and determine the degree of flattening, we need to measure more precisely the sizes of the hotspots, rather than have limits to their sizes.

3.2 3CR sources observed with larger values of n_b

Over the last few years several authors have determined the sizes of the hotspots of 3CR FR II sources from high-resolution VLA observations with n_b , the number of resolution elements along the axis of the source, in the range of about 35 to 1040 (e.g. B94; F97; Black et al. 1992; Leahy et al. 1997; Hardcastle et al. 1997). With higher values of n_b one should expect to see smaller-scale structures within the hotspots, and hence a decrease in the size of the hotspots. A linear least-squares fit to the hotspot size – n_b diagram for the B94, F97 and H98 samples exhibits a weak trend for the hotspot size to decrease with n_b with a slope of -0.15 ± 0.10 . Because of different definitions of hotspots and also difficulties in measuring their sizes, detailed comparisons are often difficult and contentious. However, the sizes of the hotspots from the B94, F97 and H98 have median values in the range of about 1.9 to 4.5 kpc and are consistent with a flattening of the hotspot size – linear size relationship beyond about 20 kpc. The knots in the jets (Table 9 of B94) are also consistent with this flattening.

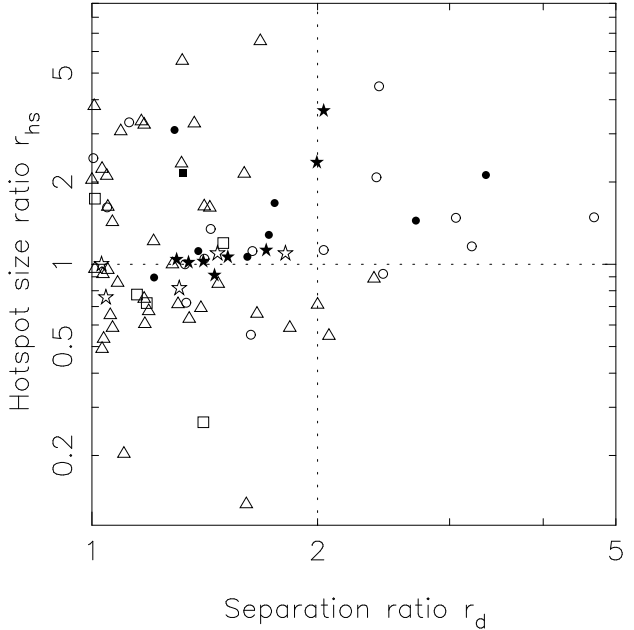


Figure 2. The ratio, r_{hs} , of the size of the hotspot farther from the radio core to that of the oppositely-directed one closer to the core, is plotted against the separation ratio, r_d , defined to be the ratio of the separations of the corresponding hotspots from the core. The open and filled circles denote galaxies and quasars from the sample of largely CSS and GPS objects (Table 1), the open and filled stars denote galaxies and quasars from B94 and F97, while the triangles represent radio galaxies from H98. Filled and open squares indicate quasars and radio galaxies from Table 2 which have not been already plotted.

3.3 Opening angle of the jets

Using the geometric mean of the major and minor axes for each hotspot and the average of the hotspots for each source, we estimate the mean opening angle, (ϕ_{obs}) , for sources below 20 kpc to be about 7° . For sources observed with at least 20 beam widths along the source axes the mean opening angle is about 5° . The estimates of the mean opening angle is roughly consistent with estimates for individual jets in different angular and linear scales. It is relevant to note that the opening angle estimated from the hotspots could, in principle, be larger than those estimated from knots in the jets because of the dentist drill effect (Scheuer 1982; Norman 1996). In the radio galaxy Cygnus A, the opening angle of the jet determined from the knots as well as the low surface brightness inter-knot regions is $\approx 1.6^\circ$ (Carilli et al. 1996), although the morphology of the jet is consistent with regions of larger opening angle of $\approx 5^\circ$ (Perley, Dreher & Cowan 1984). The jet in M87 is well-collimated on all scales out to about 2 kpc. The innermost VLBI structure indicates an opening angle of 18° , while VLA observations indicate that between the jet and knot A, the jet appears as a uniformly expanding cone with an opening angle of 7° (Biretta 1996; Biretta & Junor 1995). Among the core-dominated radio sources, one of the best studied ones is the quasar 3C345 which has an opening angle of 26° (Zensus, Cohen & Unwin 1995). Other examples are NRAO 140 with an opening angle of 12° (Marscher 1988; Unwin & Wehrle

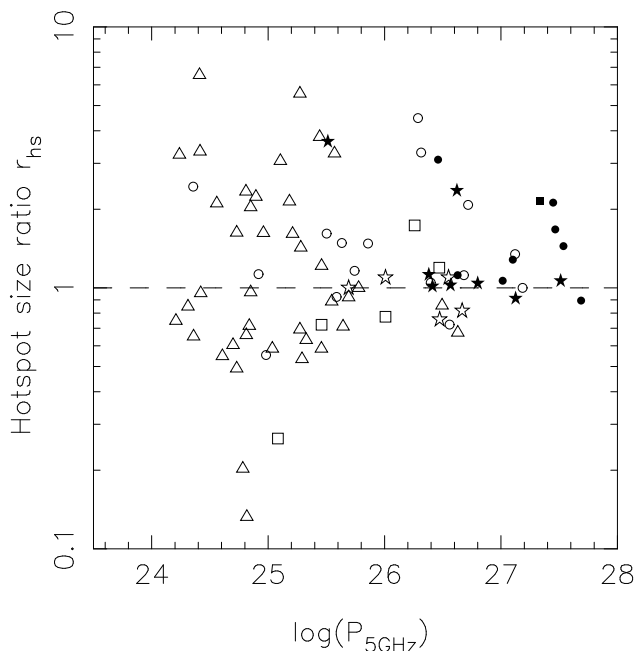


Figure 3. The ratio, r_{hs} , of the size of the hotspot farther from the radio core to that of the oppositely-directed one closer to the core, is plotted against the total luminosity at 5 GHz. The symbols are as defined in Figure 2.

1992) and 0836+710 which has a mean opening angle of 4.4° (Hummel et al. 1992).

3.4 Asymmetry in collimation

We have also examined the dependence of the ratio of the sizes of the two oppositely-directed hotspots, r_{hs} , on their relative separations from the nucleus. In Figure 2 we plot the ratio, r_{hs} , defined to be the ratio of the size of the farther hotspot to that of the nearer one, against the separation ratio, r_d , for all the sources with a detected radio core and hotspots on both sides. The separation ratio, r_d , is defined to be ≥ 1 , while r_{hs} is the ratio of the geometric mean of the corresponding hotspots. We have used only those hotspots without an upper limit to any of their axes and with a detected radio core from the sample of largely CSS and GPS objects (Table 1), the 3CR objects listed in Table 2 and the observations of B94, F97 and H98.

For the 33 high-luminosity sources with a radio luminosity at 5 GHz $\geq 10^{26}$ W Hz $^{-1}$ sr $^{-1}$, 24 have $r_{hs} > 1$, implying that the farther hotspot is larger. This trend is also seen in the most asymmetric objects, defined to be those with $r_d > 2$. Of the 12 sources with $r_d > 2$, 9 have $r_{hs} > 1$, and almost all these objects are CSSs. Either light-travel time effects or an intrinsic or environmental asymmetry can produce the effect in the observed sense. For a source inclined at about 50° to the line-of-sight and a hotspot speed of about $0.5c$, r_d is close to about 2. There have been several estimates of hotspot advance speeds in VLBI-scale double sources. O’Dea (1998) lists 7 objects which have upper limits to component proper motion which are subluminal, ranging from 0.05 – $0.5c$.

Since O’Dea’s review the upper limit for 1934–638 has been revised to $\sim 0.03 \pm 0.2c$ (Tzioumis et al. 1998), and an upper limit for 1607+26 (CTD93) has been reported to be less than $0.35c$ (Shaffer & Kellermann 1998). Current estimates of hotspot speeds suggest that the effects of an asymmetry dominate. Almost all these objects with $r_d > 2$ are compact steep spectrum radio sources, and the deficit of objects with $r_d > 2$ and $r_{hs} < 1$ is possibly a reflection of their evolution in an asymmetric environment.

The tendency for $r_{hs} > 1$ is not seen in objects of lower luminosity (Figure 3). For example, in the 50 sources with radio luminosity at 5 GHz less than 10^{26} W Hz $^{-1}$ sr $^{-1}$, only 24 have $r_{hs} > 1$. A number of these objects have r_{hs} significantly smaller than 1, which could be due to an intrinsic asymmetry in the collimation of jets on opposite sides of the nucleus.

4 DISCUSSION AND CONCLUDING REMARKS

We summarise the principal trends reported in this paper.

(i) The relationship between the hotspot sizes and the overall size of the CSS and GPS sources and studies of individual knots in the jets in these sources, suggest that they evolve in an approximately self-similar way. The hotspot size increases with distance from the core as $d_{jet} \propto l^n$ where $n \sim 1.0$ for sources smaller than about 20 kpc. This is similar for sources which have been observed with at least either 10 or 20 resolution elements, n_b , along the main axes so that the hotspots could be identified reliably.

(ii) For larger sources observed with at least either 10 or 20 resolution elements along the main axes and with a similar distribution of n_b to the sample of largely CSS and GPS sources, there appears to be a flattening of the relationship. However, since most of the sources have upper limits to their hotspot sizes the precise slope could not be determined reliably.

(iii) For samples of sources observed by Bridle et al. (1994) and Fernini et al. (1993, 1997) with n_b in the range of about 40 to 200, and a sample of 3CR sources with $z < 0.3$ summarized by Hardcastle et al. (1998) with n_b in the range of about 35 to 1040, the dependence of hotspot size on n_b is weak. The hotspot size varies by a factor of about 2 for an increase in n_b by a factor of about 300. The hotspot sizes of these large sources are consistent with a flattening of the hotspot size-linear size relationship seen for CSS and GPS objects.

(iv) There is a tendency for the farther hotspot to be larger in sources with a luminosity at 5 GHz $> 10^{26}$ W Hz $^{-1}$ sr $^{-1}$. This could be caused by both light travel time effects as well as an asymmetric environment. No such trend is seen in objects of lower luminosity where the nearer hotspot is significantly larger in a number of sources. This could be due to an asymmetry in collimation on opposite sides of the nucleus.

(v) There is a trend for the farther hotspot to be larger in the most asymmetric objects, defined to be those with $r_d > 2$. Almost all the objects with $r_d > 2$ are CSS objects. Current estimates of hotspot advance speeds suggest that these trends are due to an intrinsic asymmetry in the environment rather than light travel time effects.

In the CSS phase, the variation of the sizes of the hotspots and the widths of the knots in the jets with linear size could be due to the ambient pressure falling with distance from the nucleus, if the jet is pressure confined. The confinement of the jet by the ambient medium depends on whether the jet pressure is comparable to the external pressure. The equipartition pressure in the hotspots or knots varies from about 10^{-6} N m^{-2} on scales of a few tens of parsec to about 10^{-9} N m^{-2} at about 10 kpc from the nucleus (Fanti et al. 1995; Readhead 1995; Readhead et al. 1996a,b). For large sources, the equipartition pressure in the knots of the jets is in the range of about 10^{-10} to $10^{-12} \text{ N m}^{-2}$ (Potash and Wardle 1980; Bridle et al. 1994). Although the nature of the confining medium within about 20 kpc, i.e. the CSS phase, needs to be better understood (cf. Fanti et al. 1995), the gaseous components seen in absorption at X-ray, UV and optical wavelengths (Mathur et al. 1994; Elvis et al. 1996; Netzer 1996) could play an important role in addition to the broad-line and narrow-line gas.

For the larger FR II sources the flatter relationship seen in the present data suggests recollimation of the jets beyond the CSS phase. It is important to understand the physical process responsible for the recollimation of jets. Two interesting scenarios which have suggested for recollimation are hydrodynamic collimation involving shocks (Sanders 1983; Falle & Wilson 1985; Komissarov & Falle 1996) and magnetic collimation (Begelman, Blandford & Rees 1984; Appl & Camenzind 1992, 1993a,b; Appl 1996). The latter could provide a natural explanation of a constant width in large sources, which appears to be suggested by some of the observations such as those of B94 and F97, and in 3C353 (cf. Swain et al. 1996).

ACKNOWLEDGMENTS

We thank Robert Laing, Peter Scheuer and an anonymous referee for their critical comments and suggestions, and our colleagues at NCRA especially Gopal-Krishna and late Vijay Kapahi for their comments on this piece of work, and Judith Irwin, Ishwara-Chandra and Vasant Kulkarni for their detailed comments on the manuscript. This research has made use of the NASA/IPAC extragalactic database (NED) which is operated by the Jet Propulsion Laboratory, Caltech, under contract with the National Aeronautics and Space Administration.

REFERENCES

- Akujor C.E., Spencer R.E., Zhang F.J., Fanti C., Ludke E., Garington S.T., 1993, *A&A*, 274, 752
- Appl S., 1996, in Hardee P.E., Bridle A.H., Zensus J.A. eds., *Energy Transport in Radio Galaxies and Quasars ASP Conference Series Vol 100*, p. 129
- Appl S., Camenzind M., 1992, *A&A*, 256, 354
- Appl S., Camenzind M., 1993a, *A&A*, 270, 71
- Appl S., Camenzind M., 1993b, *A&A*, 274, 699
- Baum S.A., O'Dea C.P., Murphy D.W., de Bruyn A.G., 1990, *A&A*, 232, 19
- Begelman M.C., Blandford R.D., Rees M.J., 1984, *Rev.Mod.Phys.* 56, 255
- Biretta, J.A., 1996, in Hardee P.E., Bridle A.H., Zensus J.A. eds., *Energy Transport in Radio Galaxies and Quasars ASP Conference Series Vol 100*, p. 187
- Biretta, J.A., Junor, W., 1995, *Proc. Natl. Acad. Sci. USA*, 92, 11364
- Black A.R.S., Baum S.A., Leahy J.P., Perley R.A., Riley J.M., Scheuer P.A.G., 1992, *MNRAS*, 256, 186
- Bridle A.H., Perley R.A., 1984, *AnRA&A*, 22, 319.
- Bridle A.H., Hough D.H., Lonsdale C.J., Burns J.O., Laing R.A., 1994, *AJ*, 108, 766 (B94)
- Carilli C.L., Perley R.A., Bartel N., Sorathia B., 1996, in Hardee P.E., Bridle A.H., Zensus J.A. eds., *Energy Transport in Radio Galaxies and Quasars ASP Conference Series Vol 100*, p. 287
- Cawthorne T.V., Scheuer P.A.G., Morison I., Muxlow T.W.B., 1986, *MNRAS*, 219, 883
- Dallacasa D., Fanti C., Fanti R., Schilizzi R.T., Spencer R.E., 1995, *A&A*, 295, 27
- Elvis M., Fiore F., Giommi P., Padovani P., 1996, in *Proceedings of the Second Workshop on Gigahertz Peaked Spectrum and Compact Steep Spectrum Radio Sources*, eds. Snellen, I.A.G., Schilizzi R.T., Rottgering H.J.A., & Bremer M.N., (Leiden, Leiden Observatory), p. 193
- Falle S.A.E.G., Wilson M.J., 1985, *MNRAS*, 216, 79
- Fanaroff B.L., Riley J.M., 1974, *MNRAS*, 167, 31P
- Fanti C., Fanti R., Parma P., Venturi T., Schilizzi R.T., Nan Rendong, Spencer R.E., Muxlow T.W.B., van Breugel W., 1989, *A&A*, 217, 44
- Fanti C., Fanti R., Dallacasa D., Schilizzi R.T., Spencer R.E., Stanghellini C., 1995, *A&A*, 302, 317
- Fanti R., Fanti C., Schilizzi R.T., Spencer R.E., Rendong N., Parma P., van Breugel W.J.M., Venturi, T., 1990, *A&A*, 231, 333
- Fernini I., Burns J.O., Bridle A.H., Perley R.A., 1993, *AJ*, 105, 1690
- Fernini I., Burns J.O., Perley R.A., 1997, *AJ*, 114, 2292 (F97)
- Fey A.L., Charlot P., 1997, *ApJS*, 111, 95.
- Hardcastle M.J., Alexander P., Pooley G.G., Riley J.M., 1997, *MNRAS*, 288, 859
- Hardcastle M.J., Alexander P., Pooley G.G., Riley J.M., 1998, *MNRAS*, 296, 445 (H98)
- Hardee P.E., Bridle A.H., Zensus J.A., 1996, eds. *Energy Transport in Radio Galaxies and Quasars ASP Conference Series Vol 100*
- Hummel C.A., Muxlow T.W.B., Krichbaum T.P., Quirrenbach A., Schalinski C.J., Witzel A., Johnston K.J., 1992, *A&A*, 266, 93
- Jenkins C.J., Pooley G.G., Riley J.M., 1977, *MemRAS*, 84, 61
- Kaiser C.R., Alexander P., 1997, *MNRAS*, 286, 215
- Komissarov S.S., Falle S.A.E.G., 1996, in Hardee P.E., Bridle A.H., Zensus J.A. eds., *Energy Transport in Radio Galaxies and Quasars ASP Conference Series Vol 100*, p. 165
- Laing R.A., 1981, *MNRAS*, 195, 261
- Laing R.A., 1989, in Meisenheimer K., Roser H.J., eds. *Hot Spots in Extragalactic Radio Sources*, Springer-Verlag, p. 27
- Laing R.A., Riley J.M., Longair M.S. 1983, *MNRAS*, 204, 151
- Leahy J.P., Perley, R.A. 1995, *MNRAS* 277, 1097
- Leahy J.P., Black A.R.S., Dennett-Thorpe J., Hardcastle M.J., Komissarov S., Perley R.A., Riley J.M., Scheuer P.A.G., 1997, *MNRAS*, 291, 20
- Liu R., Pooley G.G., Riley J.M., 1992, *MNRAS*, 257, 545
- Longair M.S., 1975, *MNRAS*, 173, 309
- Lonsdale C.J., Morison I., 1983, *MNRAS*, 203, 833
- Marscher A.P., 1988, *ApJ*, 334, 552
- Mathur S., Wilkes B., Elvis M., Fiore F., 1994, *ApJ*, 434, 493
- Mutel R.L., Hodges M.W., Phillips R.B., 1985, *ApJ*, 290, 86
- Netzer H., 1996, *ApJ*, 473, 781
- Norman M.L., 1996, in Hardee P.E., Bridle A.H., Zensus J.A.

- eds., Energy Transport in Radio Galaxies and Quasars ASP Conference Series Vol 100, p. 319
- O'Dea C.P., 1998, PASP, 110, 493
- O'Dea C.P., Baum S.A., 1997, AJ, 113, 148
- Peacock J.A., Wall J.V., 1982, MNRAS, 198, 843
- Pearson T.J., Perley R.A., Readhead A.C.S., 1985, AJ, 90, 738
- Perley R.A., 1989, in Meisenheimer K., Roser H.J., eds. Hot Spots in Extragalactic Radio Sources, Springer-Verlag, p. 1
- Perley R.A., Dreher J.W., Cowan J.J., 1984, ApJ, 285, L35
- Phillips R.B., Mutel R.L., 1981, ApJ, 244, 19
- Polatidis A. G., Wilkinson P. N., Xu W., Readhead A. C. S., Pearson T. J., Taylor G. B., Vermeulen R. C., 1995, ApJS, 98, 1
- Pooley G.G., Henbest S.N. 1974, MNRAS, 169, 477
- Potash R.I., Wardle J.F.C., 1980, ApJ, 239, 42
- Readhead A.C.S., 1995, Proc. Natl. Acad. Sci. USA, 92, 11447
- Readhead A.C.S., Taylor G.B., Xu W., Pearson T.J., Wilkinson P.N., Polatidis A.G., 1996a, ApJ, 460, 612
- Readhead A.C.S., Taylor G.B., Pearson T.J., Wilkinson P.N., 1996b, ApJ, 460, 634
- Ren-dong N., Schilizzi R.T., van Breugel W.J.M., Fanti C., Fanti R., Muxlow T.W.B., Spencer R.E., 1991a, A&A, 245, 449
- Rendong N., Schilizzi R.T., Fanti C., Fanti R., 1991b, A&A, 252, 513
- Riley J.M., Pooley G.G., 1975, MemRAS, 80, 105
- Saikia D.J., Holmes G.F., Kulkarni A.R., Salter C.J., Garrington S.T., 1998, MNRAS, 298, 877
- Sanders R.H., 1983, ApJ, 266, 73
- Sanghera H.S., Saikia D.J., Lüdke E., Spencer R.E., Foulsham P.A., Akujor C.E., Tzioumis A.K., 1995, A&A, 295, 629
- Scheuer P.A.G., 1982, in eds Heesch D.S., Wade C.M., IAU Symp 97: Extragalactic Radio Sources, Reidel, Dordrecht, p. 163
- Shaffer D.B., Kellermann K.I., 1998, in Zensus J.A., Taylor G.B., Wrobel J.M., eds, Radio emission from galactic and extragalactic compact sources, ASP conference series vol 144, San Francisco, USA, p. 191
- Simon R.S., Readhead A.C.S., Moffet A.T., Wilkinson P.N., Booth R., Allen B., Burke B.F., 1990, ApJ, 354, 140
- Spencer R.E., McDowell J.C., Charlesworth M., Fanti C., Parma P., Peacock J.A., 1989, MNRAS, 240, 657
- Spencer R.E., Schilizzi R.T., Fanti C., Fanti R., Parma P., van Breugel W.J.M., Venturi T., Muxlow T.W.B., Nan Rendong, 1991, MNRAS, 250, 225
- Stanghellini C., O'Dea C.P., Baum S.A., & Fanti R., 1990, in Proceedings of the Dwingeloo workshop on Compact Steep Spectrum and GHz Peaked Spectrum Radio Sources, eds. Fanti C., Fanti R., O'Dea C.P., & Schilizzi R.T., Istituto di Radioastronomia, Bologna, p. 17
- Stanghellini C., Dallacasa D., O'Dea C.P., Baum S.A., Fanti R., & Fanti C., 1996, in Proceedings of The Second Workshop on Gigahertz Peaked Spectrum and Compact Steep Spectrum Radio Sources, eds. Snellen, I.A.G., Schilizzi R.T., Rottgering H.J.A., & Bremer M.N., Leiden Observatory, Leiden, p. 4
- Stanghellini C., O'Dea C.P., Baum S.A., Dallacasa D., Fanti R., Fanti C., 1997, A&A, 325, 943
- Swain M.R., Bridle A.H., Baum S.A., 1996, in Hardee P.E., Bridle A.H., Zensus J.A. eds., Energy Transport in Radio Galaxies and Quasars ASP Conference Series Vol 100, p. 299
- Taylor G.B., Vermeulen R.C., Pearson T.J., 1995, Proc. Natl. Acad. Sci. USA, 92, 11381
- Taylor G.B., Readhead A.C.S., Pearson T.J., 1996, ApJ, 463, 95
- Tzioumis A.K. et al., 1998, in Zensus J.A., Taylor G.B., Wrobel J.M., eds, Radio emission from galactic and extragalactic compact sources, ASP conference series vol 144, San Francisco, USA, p. 179
- Unwin, S.C., & Wehrle, A.E., 1992, ApJ, 398, 74
- van Breugel W. J. M., Fanti C., Fanti R., Stanghellini C., Schilizzi R.T., Spencer R.E., 1992, A&A, 256, 56
- Wilkinson P.N., Tzioumis A.K., Benson J.M., Walker R.C., Simon R.S., Kahn F.D., 1991, Nature, 352, 313
- Zensus J.A., Cohen M.H., Unwin S.C., 1995, ApJ, 443, 35